El Niño-Induced Tropical Ocean / Land Energy Exchange in MERRA-2 and M2AMIP

Michael G. Bosilovich[1] and Franklin R. Robertson[2]

[1]GMAO NASA GSFC, Code 610.1, Greenbelt, MD; [2]NASA MSFC Earth Sciences Division

GMAO
Global Modeling & Assimilation Office

Motivation

Surface temperature variations between the tropical land and ocean are known to be highly correlated. In this paper, we evaluate the processes of temperature variation around the topics with MERRA-2 and its model experiment M2AMIP (as well as observations when present). The reanalysis provides atmospheric quantities not easily observed (horizontal transport and vertical motions) while the model ensemble provides insight into SST forcing with internal atmospheric variability minimized. Of particular interest is the connection of El Niño to the Global Monsoon regions in the tropics (30S – 30N).

Data and Methods

- MERRA-2: Gelaro et al. (2017)
- M2AMIP: Uses the same model and climate forcing, including SST as MERRA-2. 10-members ensemble mean. Collow et al. (2017)
- Observations: CRU (Harris et al. 2014), GEWEX Surface Radiation Budget (3.0 Zhang et al. 2009)
- Composite El Niño
  - Find the peak surface temperature in the Niño34 region
  - Collect data for each of 8 peaks +-12 months from the peak, computing mean and st. dev.
- Global Monsoon Region: (e.g. Wang et al. 2012)

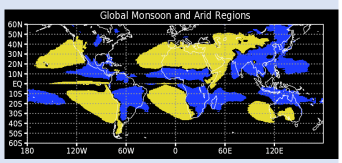

Time Series

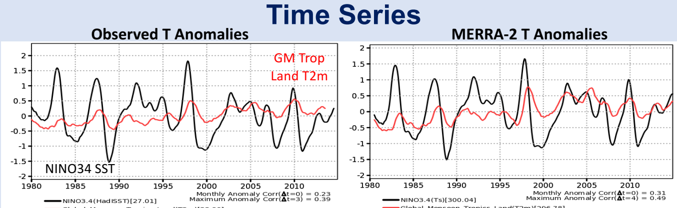

Above: De-seasonalized detrended temperature anomalies for NINO34 and Global Monsoon Land regions in observations and MERRA-2, showing lag of the land warming behind the SST warming.

- Composite El Niño centers DEC1982, AUG1987, JAN1992, DEC1994, DEC1997, NOV2002, NOV2006, DEC2009

Using CRU T2m and HadISST, we characterize the correlation of the Niño 3.4 SST with global land temperatures. MERRA-2 establishes a reasonable connection to most regions, except central Africa, while the ensemble mean M2AMIP shows very strong connections to most regions in the observations, except Africa. This lack of correlation is shown not related to El Niño.

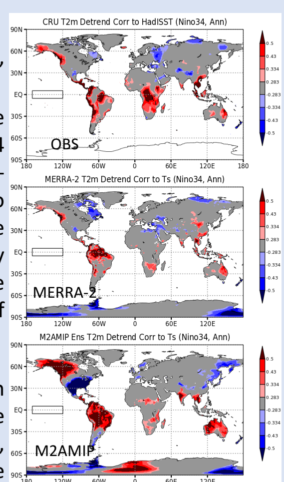

Right: Temporal correlation map of SST in the NINO34 region and 2m air temperature over land. HadISST is correlated to CRU, while MERRA-2 and M2AMIP use the MERRA-2 merged SST (these are lag=0).

Composite El Niño

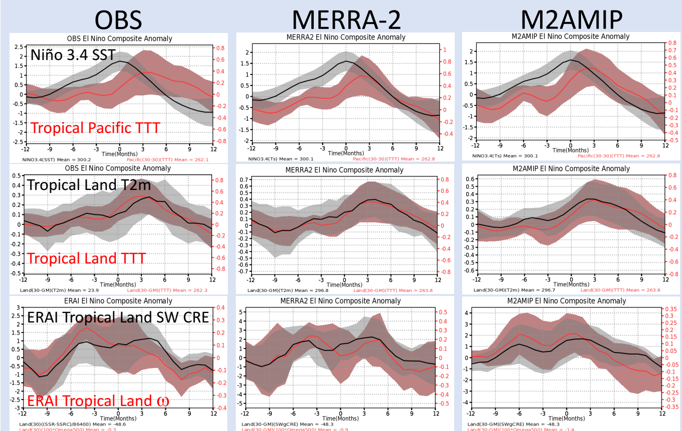

Above: Composite area average time series of Observations (left) MERRA-2 (center) M2AMIP (right) for Niño 3.4 surface temperature and near surface air temperature (top), Tropical land T2m and TTT (middle), SWCRE and pressure velocity (bottom). The time series of monthly means have been deseasonalized and detrended. Shaded areas represent +/-1 standard deviation. Here, Tropics are bounded by 30S-30N, and the land regions are within the defined Global Monsoon area. ERA-Interim (Dee et al. 2011) replaces observations in the lower left as a point of comparison.

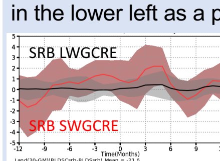

Above: SRB Composite cloud effects on the tropical global monsoon land areas. The effect of clouds is more significant in shortwave

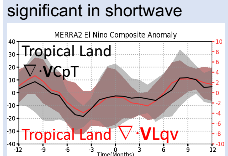

Above: MERRA-2 vertically integrated CpT and Lqv convergence over all tropical land, representing the transport of heat and moisture toward the land surface.

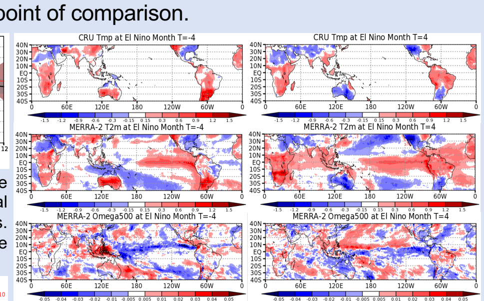

Above: Composite maps 4 months before (left) and 4 months after (right) peak El Niño SST. MERRA-2 land temperature anomalies reasonably compare to those of CRU (despite areas of low correlation mentioned previously). The composite vertical velocity is also compared showing the locations of subsidence regions over the tropical continents. Omega is positive downward, so that red values show reduced upward or increased downward motion.

Summary

While indeed the El Niño circulation is complicated and varies from one event to the next, composite analysis shows some systematic features coupling the circulation from the ocean to the land. Warming across the tropical land areas generally lags behind the warming of the oceans, but some areas can noticeably warm along with the event, associated with a shift in the atmospheric circulation including less heat convergence over land and reduced upward motion or increased subsidence. This circulation permits atmospheric warming and land surface warming from the reduced cloud effect on shortwave radiation. With only eight events in the reanalysis period, there is substantial variance in the sample.

Collow, A. and co-authors, 2017: File Specification for MERRA-2 AMIP. Available at https://gmao.gsfc.nasa.gov/reanalysis/MERRA-2/docs/.
Dee, D. P., et al., 2011: The ERA-Interim reanalysis: configuration and performance of the data assimilation system. Q.J.R. Meteorol. Soc., 137, 553–597. doi:10.1002/qj.828.
Gelaro, R., 2017: The Modern-Era Retrospective Analysis for Research and Applications, Version 2 (MERRA-2). J. Climate, 30, 5419–5454, doi:10.1175/JCLI-D-16-0758.1.
Harris, I., Jones, P.D., Osborn, T.J. and Lister, D.H., 2014: Updated high-resolution grids of monthly climatic observations – the CRU TS3.10 Dataset. Int. J. Climatol., 34: 623–642. doi:10.1002/joc.3711
Wang, B., Liu, J., Kim, H.J., Webster, P.J. and Yim, S.Y., 2012. Recent change of the global monsoon precipitation (1979–2008). *Climate Dynamics*, *39*(5), pp.1123-1135. DOI 10.1007/s00382-011-1266-z
Zhang, T., P. W. Stackhouse, S. K. Gupta, S. J. Cox, and J. C. Mikovitz, 2009: Validation and Analysis of the Release 3.0 of the NASA GEWEX Surface Radiation Budget Dataset, AIP Conference Proceedings 1100:1, 597-600.

E-mail: Michael.Bosilovich@nasa.gov | *Web:* gmao.gsfc.nasa.gov

National Aeronautics and Space Administration